Progress In Electromagnetics Research, PIER 80, 447–460, 2008

APPLICATION OF SYNTHETIC BANDWIDTH APPROACH IN SAR POLAR FORMAT ALGORITHM USING THE DERAMP TECHNIQUE

X. Nie, D.-Y. Zhu, and Z.-D. Zhu

Nanjing University of Aeronautics & Astronautics
Nanjing 210016, China

Abstract—The problem of wide bandwidth management in ultra-high resolution SAR systems can be solved by adopting stepped chirps and applying synthetic bandwidth approach. However, high resolution SAR image formation is a non-separable 2-D impulse compression processing, so the synthetic bandwidth procedure should be modified correspondingly with the image formation algorithm adopted. This paper demonstrates the application of synthetic bandwidth approach in SAR Polar Format Algorithm (PFA) using the deramp technique. The problem of motion compensation between the sub-pulses within a burst is discussed, and the signal processing flows are investigated in detail. The presented approach is validated by point target simulation.

1. INTRODUCTION

The Synthetic Aperture Radar (SAR) is an all-weather imaging tool that achieves fine along-track resolution by taking the advantage of radar motion to synthesize a large antenna aperture [1]. The basic principle of Synthetic Aperture Radar (SAR) has been outlined in reference [2, 3]. SAR has been shown to be very useful over a wide range of applications, including target detection [4], target discrimination [5, 6], target recognition [7], velocities measurement [8], identification of landmine-like objects [9, 10], snow monitoring [11], classification of earth terrain [12] etc.

There is a growing demand for SAR systems with an ultra-high resolution in the recent couple of years. In Germany FGAN-FHR has built up an experimental system: PAMIR [13–18], the Phased Array Multifunctional Imaging Radar with the very high resolution in the order of one decimeter. Range resolution is determined by the bandwidth of the transmitted pulse, so for such a resolution, the

transmitted bandwidth has to be at least 1.8 GHz. The need for such a large bandwidth leads to a lot of problems to be solved. One problem is the broadband beam-former for the phased array with the need for a great number of switchable true time delays (TTD). And the antenna has to have excellent transient response for ultra wideband (UWB) signals [19]. Also the generation of wideband waveforms and the construction of the receivers with high speed A/D-converters are nontrivial engineering tasks. Therefore, it would be a good choice to adopt stepped chirps to reduce the instantaneous bandwidth and sampling rate requirements of the radar system. It means that the total wide bandwidth is split over a certain number of pulses with relative narrow bandwidth (sub-pulses) belonging to one burst. A series of bursts of these narrowband pulses are transmitted. Adequate post-processing is required to process the received signals to form an image with high resolution. Some methods are purposely for dealing with the stepped chirps to form an image [20, 21], but the most common and simple processing way is using the synthetic bandwidth technique to realize the combination of the sub-bands first, and then processing the synthesized signal with existing standard SAR image formation algorithms.

Bandwidth synthesis can be completed either in the time domain [22] or in the frequency domain [23], or by using the deramp technique [24] which will be discussed in the following. There is a limit for swath width while using deramp technique, but a method to make the technique applicable for arbitrary wide swath has been demonstrated in [25, 26].

In the next section, the waveform model of stepped chirps in SAR is given, and the received signal when using deramp technique is formulated. The relative motion between the radar and target from one sub-pulse to another within a burst is considered, and the compensation method is discussed in Section 3. In Section 4, the application of synthetic bandwidth approach in SAR Polar Format Algorithm (PFA) using the deramp technique is demonstrated, and the signal processing flows are discussed in detail. Simulation results validating the presented approach are shown in Section 5.

2. WAVEFORM MODELING

Figure 1 indicates the signal frequency variety of the transmitted stepped chirps in SAR as a function of time. Assume that the step number is N, the time interval between two subsequent sub-chirps is PRI, and the N sub-chirps belonging to one burst are used to construct a single wide-bandwidth chirp with centre frequency f_c, total

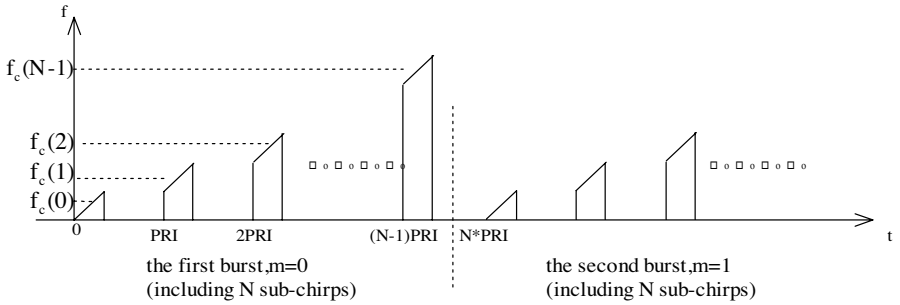

Figure 1. The frequency diversity of the transmitted stepped chirps in SAR.

bandwidth B, chirp rate γ and pulse duration T_p, then the centre frequency of the sub-chirps should be stepped by a constant increment f_{step} to cover the whole synthesized bandwidth, where $f_{step} = \frac{B}{N}$. Therefore, the center frequency of the kth ($k = 0, 1, 2, \ldots, N-1$) sub-chirp is given by

$$f_c(k) = f_c + (k + 1/2 - N/2) f_{step}. \tag{1}$$

Here define

$$\Delta f_k = (k + 1/2 - N/2) f_{step} \tag{2}$$

Each sub-chirp should have bandwidth $B_n = f_{step}$, chirp rate γ, pulse duration $T_{pn} = \frac{T_p}{N}$, and the baseband chirp signal is formulated as:

$$p(\tau) = \text{rect}\left(\frac{\tau}{T_{pn}}\right) \exp\left[j\pi\gamma\tau^2\right] \tag{3}$$

where τ is the fast (range) time, and $\text{rect}(\frac{\tau}{T_{pn}})$ represents a rectangular function of duration T_{pn} centered at $\tau = 0$.

In spotlight SAR, a SAR sensor mounted on a moving platform traveling a relatively linear path at a fixed velocity transmits a series of the bursts of the narrow-bandwidth chirps defined above to illuminate a target area. Assume the burst number is L. The kth ($k = 0, 1, 2, \ldots, N-1$) sub-chirp belonging to the mth ($m \leq L$) burst is expressed as

$$s_t(\tau, k; m) = \text{rect}\left(\frac{\tau}{T_{pn}}\right) \exp\left[j2\pi f_c(k)\tau\right] \exp\left[j\pi\gamma\tau^2\right] \tag{4}$$

Assume there is a specific point target j in the illuminated area, and the instantaneous distance between it and the antenna phase center

(APC) at this sub-chirp's transmission time is marked as $r_j(k;m)$. The demodulated echo signal backscattered from target j has the form

$$\begin{aligned} s_b(\tau,k;m) \;=\; & \mathrm{rect}(\frac{\tau-2r_j(k;m)/c}{T_{pn}})\exp\left[-j2\pi f_c(k)\frac{2r_j(k;m)}{c}\right] \\ & \exp\left[j\pi\gamma(\tau-\frac{2r_j(k;m)}{c})^2\right] \end{aligned} \tag{5}$$

where c is the speed of light.

While the deramp-on-receive approach is employed, the reference signal for mixing is

$$s_{ref}(\tau,k;m)=\exp\left[j\pi\gamma\left(\tau-\frac{2r_{ref}(k;m)}{c}\right)^2\right] \tag{6}$$

where $r_{ref}(k;m)$ represents the instantaneous distance between the APC and the reference point target (typically the scene center point) at the same sub-chirp transmission time.

The deramped signal that results from mixing the received signal of (5) and the complex conjugate of the reference function of (6) is only dechirped in range and is a mono-frequency signal formulated as

$$\begin{aligned} s_{de}(\tau,k;m) =& \mathrm{rect}\left(\frac{\tau-2r_j(k;m)/c}{T_{pn}}\right)\exp\left[-j4\pi f_c(k)\frac{r_j(k;m)}{c}\right. \\ & \left.+j\pi\gamma\left(\tau-\frac{2r_j(k;m)}{c}\right)^2-j\pi\gamma\left(\tau-\frac{2r_{ref}(k;m)}{c}\right)^2\right] \\ =& \mathrm{rect}\left(\frac{\tau-2r_j(k;m)/c}{T_{pn}}\right)\exp\left\{j2\pi\gamma\left[\left(\frac{2r_{ref}(k;m)}{c}\right.\right.\right. \\ & \left.\left.\left.-\frac{2r_j(k;m)}{c}\right)\tau\right]-j4\pi f_c(k)\frac{r_j(k;m)}{c}\right. \\ & \left.+j\pi\gamma\left[\left(\frac{2r_j(k;m)}{c}\right)^2-\left(\frac{2r_{ref}(k;m)}{c}\right)^2\right]\right\} \end{aligned} \tag{7}$$

and the frequency is slant range dependent since targets at different ranges correspond to different frequencies.

After applying the deramp technique to the sub-pulses one by one, the mono-frequency sub-signals are prepared for the concatenation via the synthetic bandwidth approach.

3. COMPENSATION OF THE RELATIVE MOTION BETWEEN SUB-PULSES WITHIN A BURST

The bandwidth synthesis starts with (7), but before the synthetic bandwidth technique is applied, it should be declared that synthetic bandwidth theory requires that the range between the APC and each target should be fixed within a burst, i.e., $r_j(k;m)$ and $r_{ref}(k;m)$ in (7) should have fixed values for a certain 'm' regardless of k. Nevertheless, SAR sensor moves along with the carrier and both $r_j(k;m)$ and $r_{ref}(k;m)$ change with k from sub-pulse to sub-pulse. If the$N$ sub-pulses were combined directly, that would cause much error. Therefore, this change in range from one sub-pulse to another should be accounted for and compensated first.

However, for different point targets in different locations, this change in range between sub-pulses is different, i.e., this change is space-variant. Therefore, it is difficult to compensate for the change completely point by point. We can merely choose to do a space-invariant compensation to all targets according to the relative motion between the APC and the reference point target, i.e., do the compensation according to $r_{ref}(k;m)$.

Within a burst, we choose to compensate each sub-pulse' transmission location to the first sub-pulse' ($k = 0$) transmission location. It means $r_{ref}(0;m)$ is chosen as the reference range for the mth burst, and the compensation is done sub-pulse by sub-pulse according to the difference between $r_{ref}(0;m)$ and $r_{ref}(k;m)$ for each k, including time-shift and phase compensation. The appropriate time-shift is given by

$$\Delta t_{location}(k;m) = \frac{2[r_{ref}(0;m) - r_{ref}(k;m)]}{c} \tag{8}$$

and the phase compensation factor is given by

$$\phi_{location}(k,m) = \exp\left[j4\pi f_c(k)\frac{r_{ref}(k;m) - r_{ref}(0;m)}{c}\right] \tag{9}$$

Although this compensation is only exact for the reference point target, it might be adequate for all targets in the illuminated area when the imaged scene radius is selected to limit the quadratic phase error induced by range curvature within $\pi/2$ [27].

Afterwards, it is appropriate to assume that the SAR sensor doesn't move within a burst, but stops at the transmission location of the first sub-pulse transmitting the N sub-pulses within this burst one by one, and then moves to next position to transmit next burst of sub-pulses. After the compensation is done to (7), all $r_j(k;m)$

and $r_{ref}(k;m)$ in (7) can be substituted by $r_j(0;m)$ and $r_{ref}(0;m)$ respectively, and (7) is changed to

$$\begin{aligned} s_{de\_loc}(\tau,k;m) \;=\; & \mathrm{rect}\left(\frac{\tau-2r_j(0;m)/c}{T_{pn}}\right)\exp\left\{j\pi\gamma\left[2\tau\left(\frac{2r_{ref}(0;m)}{c}\right.\right.\right. \\ & \left.\left.\left.-\frac{2r_j(0;m)}{c}\right)\right]-j4\pi f_c(k)\frac{r_j(0;m)}{c}\right. \\ & \left.+j\pi\gamma\left[\left(\frac{2r_j(0;m)}{c}\right)^2-\left(\frac{2r_{ref}(0;m)}{c}\right)^2\right]\right\} \end{aligned} \tag{10}$$

4. THE APPLICATION OF SYNTHETIC BANDWIDTH APPROACH IN SAR POLAR FORMAT ALGORITHM

After the compensation of the relative motion between sub-pulses within a burst, synthetic bandwidth approach can be applied to combine the N sub-pulses ($k = 0, 1, 2, \ldots, N-1$) in virtue of Equation (10). The N mono-frequency sub-pulses within a burst can be concatenated to a long mono-frequency signal via two steps, time-shift and superposition. (For simplicity, the common argument m is omitted in the following expression). Denote

$$\phi_j = j\pi\gamma\left[\left(\frac{2r_j(0)}{c}\right)^2-\left(\frac{2r_{ref}(0)}{c}\right)^2\right] \tag{11}$$

Reset the phase terms in (10) [24, 25], it can be formulated as

$$\begin{aligned} s_{de\_loc}(\tau,k) \;=\; & \mathrm{rect}\left(\frac{\tau-2r_j(0)/c}{T_{pn}}\right)\exp\left\{j2\pi\left[\gamma\frac{2r_{ref}(0)}{c}\tau\right.\right. \\ & \left.\left.-\gamma\frac{2r_j(0)}{c}\left(\tau+\frac{f_c(k)}{\gamma}\right)\right]+\phi_j\right\} \end{aligned} \tag{12}$$

It has to be shifted in the time-domain by

$$\Delta t(k) = \frac{\Delta f_k}{\gamma} \tag{13}$$

Using the expression $\Delta f_k = (k+\frac{1}{2}-\frac{N}{2})B_n$, $B_n = \gamma T_{pn}$ and $f_c(k) =$

$f_c + \Delta f_k$, the time-shifted version of Equation (12) becomes

$$\begin{aligned} s_1(\tau, k) &= s_{de\_loc}\left(\tau - \frac{\Delta f_k}{\gamma}, k\right) \\ &= \mathrm{rect}\left(\frac{\tau - (k + 1/2 - N/2)T_{pn} - 2r_j(0)/c}{T_{pn}}\right) \\ &\quad \exp\left\{j2\pi\left[\gamma\frac{2r_{ref}(0)}{c}\tau - \gamma\frac{2r_j(0)}{c}\left(\tau + \frac{f_c}{\gamma}\right) - \Delta f_k\frac{2r_{ref}(0)}{c}\right] + \phi_j\right\} \end{aligned} \quad (14)$$

It can be noticed that there is only one phase term different for each sub-pulse

$$\exp\left[j2\pi\Delta f_k\frac{2r_{ref}(0)}{c}\right] \quad (15)$$

If this phase term is compensated, different sub-pulses in this burst would have exactly the same expression except the rect$(\cdot)$ function part. Considering about the azimuth processing in PFA afterwards, the phase compensation factor is chosen as

$$\phi(k) = \exp\left(j2\pi f_c(k)\frac{2r_{ref}(0)}{c}\right) \quad (16)$$

for the purpose of doing azimuth dechirp at the same time, and this is the key point to apply synthetic bandwidth approach to PFA. After multiplying (14) by $\phi(k)$, the signal becomes

$$\begin{aligned} s_2(\tau, k) &= s_1(\tau, k) * \phi(k) \\ &= \mathrm{rect}\left(\frac{\tau - (k + 1/2 - N/2)T_{pn} - 2r_j(0)/c}{T_{pn}}\right) \\ &\quad \exp\left\{j2\pi\left[\gamma\frac{2r_{ref}(0)}{c}\tau - \gamma\frac{2r_j(0)}{c}\left(\tau + \frac{f_c}{\gamma}\right)\right.\right. \\ &\quad \left.\left. + f_c\frac{2r_{ref}(0)}{c}\right] + \phi_j\right\} \end{aligned} \quad (17)$$

It is obvious that two neighboring sub-pulses have exactly the same phase term, and they are just aligned having neither overlap nor gap in time. Each sub-pulse lasts for a period of T_{pn}, and two neighboring sub-pulses are shifted in time by T_{pn}. Thus, all of the N

sub-pulses in a burst can be added linearly

$$\begin{aligned} s_{syn}(\tau) &= \sum_{k=0}^{N-1} s_2(\tau, k) \\ &= \text{rect}\left(\frac{\tau - 2r_j(0)/c}{NT_{pn}}\right) \exp\left\{j2\pi\left[\gamma\left(\frac{2r_{ref}(0)}{c} - \frac{2r_j(0)}{c}\right)\tau \right.\right. \\ &\quad \left.\left. + f_c\left(\frac{2r_{ref}(0)}{c} - \frac{2r_j(0)}{c}\right)\right] + \phi_j\right\} \end{aligned} \tag{18}$$

The bandwidth synthesis is completed till this step. N sub-pulses within a burst are synthesized to one single signal. The synthetic signal is still a mono-frequency signal in range, but the duration is N times longer, which brings the improvement of range resolution which is N times higher.

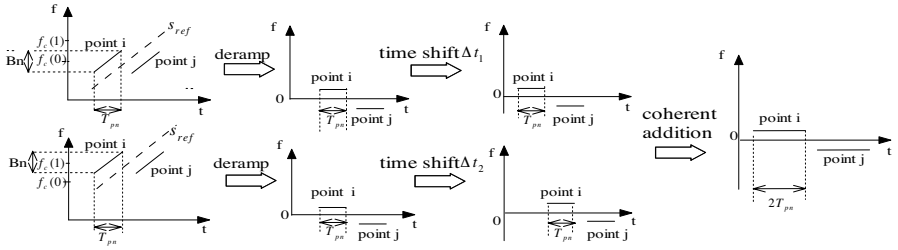

Figure 2. Graphical explanation of the signal concatenation (for $N = 2$).

Figure 2 takes $N = 2$ as an example and indicates the graphical explanation of signal concatenation for two point targets i, j at different ranges. Two mono-frequency signals were synthesized corresponding to these two targets respectively. Note the frequency-dependent skew in time, which has to be handled afterwards.

Notice that (18) can be formulated as

$$\begin{aligned} s_{syn}(\tau; m) = \text{rect}\left(\frac{\tau - 2r_j(0;m)/c}{NT_{pn}}\right) \exp\left\{j\frac{4\pi\gamma}{c}\left[\frac{f_c}{\gamma} + \tau - \frac{2r_{ref}(0;m)}{c}\right]\right. \\ \left.[r_j(0;m) - r_{ref}(0;m)] + j\frac{4\pi\gamma}{c^2}\left[r_j(0;m) - r_{ref}(0;m)\right]^2\right\} \end{aligned} \tag{19}$$

in which the argument m is displayed again. It is clear and desirable that a signal dechirped both in range and azimuth is constructed, which shows that the bandwidth synthesis process not only accomplishes the signal concatenation but also accomplishes dechirp in azimuth as well.

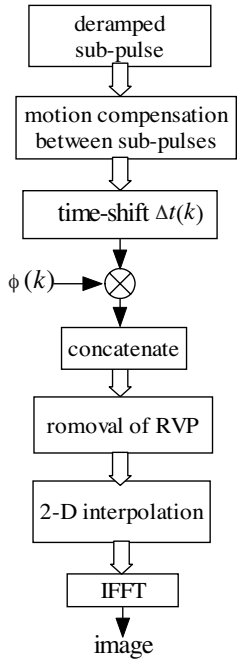

Figure 3. The flow chart.

After the bandwidth synthesis approach is executed to the L bursts one by one, L dechirped signals are synthesized which can be processed directly by PFA. But the last phase term in (19) has to be handled first before polar formatting. This phase term is called Residual Video Phase (RVP), and it would cause distortion to image when the illuminated area is large or the resolution is high. So the removal of RVP should be done first. The problem of frequency-dependent skew discussed above can also be solved via this procedure, and the echoes returned from different ranges are aligned, which is referred to as the range deskew. Then, the data can be stored in the polar format, followed by the 2-D interpolation. Finally, 2-D IFFT will convert the data into the 2-D focused image.

5. SIMULATION RESULTS

In this section, point target simulation is employed to validate the presented approach. A spotlight SAR system adopting stepped chirps in the step of 4 ($N = 4$) and operating in the broadside imaging geometry is assumed. Echo signals with deramp-on-receive are

Table 1. Parameters in the simulation.

Step number	Total bandwidth	Sub bandwidth	Frequency step size	Center frequency	Sub-chirp center frequency	Scene radius
4	1.5 GHz	375 MHz	375 MHz	10 GHz	9.4375 G-1.05625 G	88 m

simulated. Parameters outlining the simulation are listed in Table 1.

According to the parameters above, the theoretical resolution should be $0.1 * 0.1$ m.(azimuth*range). The imaged scene radius is selected to limit the quadratic phase error induced by range curvature within $\pi/2$ [27], and 9 point targets are assumed to be distributed as Fig. 4 indicates.

The processed image via the presented approach is shown in Fig. 5. The impulse response function(IRF) in range and azimuth of two selected point targets, point O in the scene center and point A on

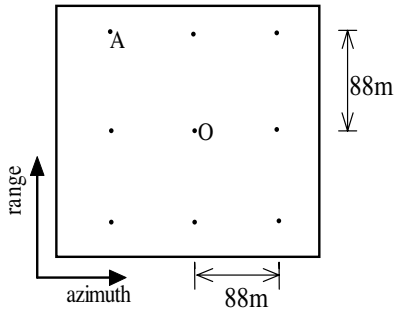

Figure 4. Simulated scene geometry.

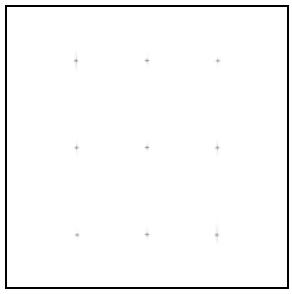

Figure 5. SAR image processed with PFA.

the scene border in the upper left corner, are presented in Fig. 6 and Fig. 7. Table 2 summarizes the measured resolutions and Integrated Sidelobe Ratio (ISLR), Peak Sidelobe Ratio (PSLR) in both range and azimuth dimension.

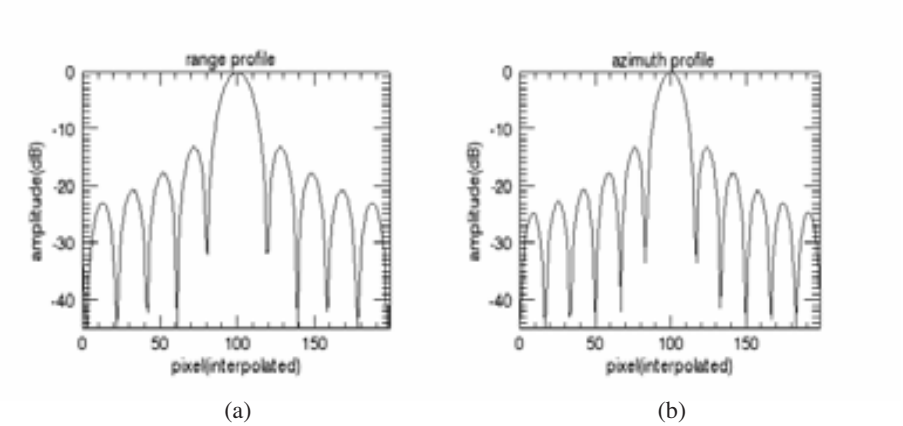

(a) (b)

Figure 6. Impulse response function of the point at the scene center, (a) range profile, (b) azimuth profile.

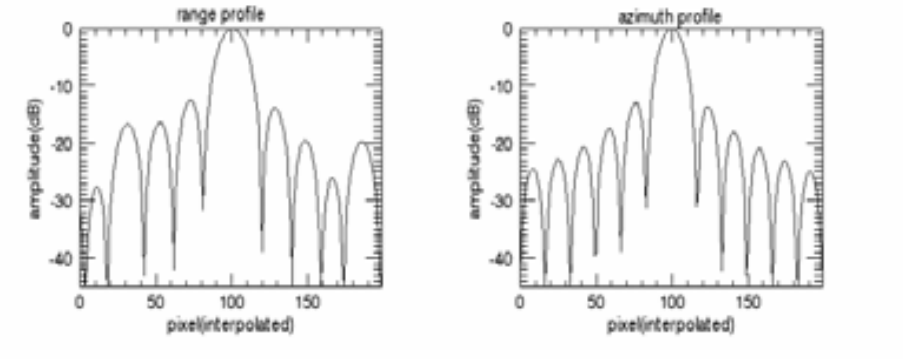

(a) (b)

Figure 7. Impulse response function of the point on the scene border, (a) range profile, (b) azimuth profile.

It can be observed that the focusing is nearly perfect for the point at the scene center corresponding to the theoretical values, and slightly distorted in range for the point on the scene border as its range profile appears slightly non-symmetrical in Fig. 7(a). This is resulted from the motion compensation between sub-pulses within a burst, which is only exact for the scene center point. However, the distortion is not

Table 2. Point target impulse response characteristics.

	Point at the scene center		Point on the scene border	
	Range	Azimuth	Range	Azimuth
Resolution measured	0.0923	0.1059	0.0974	0.0993
ISLR (dB)	□9.96297	-□9.86119	□9.45427	□8.76849
PSLR (dB)	□13.2334	- 13.2684	□12.5496	□12.0572

serious at all, and the simulation results prove that the application of synthetic bandwidth approach in SAR Polar Format Algorithm using deramp technique is feasible.

6. CONCLUSIONS

In this paper, the application of synthetic bandwidth approach in the Polar Format Algorithm in spotlight SAR using deramp technique is demonstrated. The relative motion between the APC and targets from one sub-pulse to another within a burst is considered first and the compensation method is discussed. The signal processing flow of the application is induced in detail. The presented approach is validated by point target simulation finally.

REFERENCES

1. Skolnik, M. I., *Radar Handbook*, McGraw-Hill, New York, 1970.
2. Chan, Y. K. and V. C. Koo, "An introduction to Synthetic Aperture Radar (SAR)," *Progress In Electromagnetics Research B*, Vol. 2, 27–60, 2008.
3. Chan, Y. K. and S. Y. Lim, "Synthetic Aperture Radar (SAR) signal generation," *Progress In Electromagnetics Research B*, Vol. 1, 269–290, 2008.
4. Xue, W. and X.-W. Sun, "Target detection of vehicle volume detecting radar based on wigner-hough transform," *Journal of Electromagnetic Waves and Applications*, Vol. 21, No. 11, 1513–1523, 2007.
5. Lee, J. H. and H. T. Kim, "Radar target discrimination using transient response reconstruction," *Journal of Electromagnetic Waves and Applications*, Vol. 19, No. 5, 655–669, 2005.

6. Jung, J. H., H. T. Kim, and K. T. Kim, "Comparisons of four feature extraction approaches based on Fisher's linear discriminant criterion in radar target recognition," *Journal of Electromagnetic Waves and Applications*, Vol. 21, No. 2, 251–265, 2007.
7. Seo, D.-K., K. T. Kim, I. S. Choi, and H. T. Kim, "Wide-angle radar target recognition with subclass concept," *Progress In Electromagnetics Research*, PIER 44, 231–248, 2004.
8. Wang, C. J., B. Y. Wen, Z. G. Ma, W. D. Yan, and X. J. Huang, "Measurement of river surface currents with UHF FMCW radar systems," *Journal of Electromagnetic Waves and Applications*, Vol. 21, No. 3, 375–386, 2007.
9. Nishimoto, M., S. Ueno, and Y. Kimura, "Feature extraction from GPR data for identification of landmine-like objects under rough ground surface," *Journal of Electromagnetic Waves and Applications*, Vol. 20, No. 12, 1577–1586, 2006.
10. Van den Bosch, I., S. Lambot, M. Acheroy, I. Huynen, and P. Druyts, "Accurate and efficient modeling of monostatic GPR signal of dielectric targets buried in stratified media," *Progress In Electromagnetics Research Symposium*, Hangzhou, China, August 22–26, 2005.
11. Storvold, R., E. Malnes, Y. Larsen, K. A. Hogda, S.-E. Hamran, K. Mueller, and K. Langley, "SAR remote sensing of snow parameters in norwegian areas — Current status and future perspective," *Journal of Electromagnetic Waves and Applications*, Vol. 20, No. 13, 1751–1759, 2006.
12. Kong, J. A., S. H. Yueh, H. H. Lim, R. T. Shin, and J. J. van Zyl, "Classification of earth terrain using polarimetric synthetic aperture radar images," *Progress In Electromagnetics Research*, PIER 03, 327–370, 1990.
13. Ender, J. H. G. and A. R. Brenner, "PAMIR-a wideband phased array SAR/MTI system," *Radar, Sonar and Navigation, IEE Proceedings*, Vol. 150, No. 3, 165–172, 2003.
14. Brenner, A. R. and J. H. G. Ender, "First experimental results achieved with the new very wideband SAR system PAMIR," *Processing of EUSAR*, 81–86, VDE, Germany, 2002.
15. Cantalloube, H. and P. Dubois-Fernandez, "Airborne X-band SAR imaging with 10 cm resolution: Technical challenge and preliminary results," *Radar, Sonar and Navigation, IEE Proceedings*, Vol. 153, 163–176, 2006.
16. Brenner, A. R. and J. H. G. Ender, "Airborne SAR imaging with subdecimeter resolution," *Processing of EUSAR*, 267–270, VDE,

Germany, 2004.

17. Brenner, A. R. and J. H. G. Ender, "Very wideband radar imaging with the airborne SAR sensor PAMIR," *IGARSS '03 Proceedings. 2003 IEEE International*, Vol. 1, 533–535, 2003.
18. Brenner, A. R. and J. H. G. Ender, "Demonstration of advanced reconnaissance techniques with the airborne SAR/GMTI sensor PAMIR," *Radar, Sonar and Navigation, IEE Proceedings*, Vol. 153, No. 2, 152–162, April 2006.
19. Gopikrishna, M., D. D. Krishna, A. R. Chandran, and C. K. Aanandan, "Square monopole antenna for ultra wide band communication applications," *Journal of Electromagnetic Waves and Applications*, Vol. 21, No. 11, 1525–1537, 2007.
20. Scheiber, R., F. Barbosa, A. Nottensteiner, and R. Horn, "E-SAR upgrade to stepped-frequency mode: System description and data processing approach," *Processing of EUSAR*, Germany, May 2006.
21. Doerry, A. W., *SAR Processing with Stepped Chirps and Phased Array Antennas*, Sandia National Laboratories, Sept. 2006.
22. Lord, R. T. and M. R. Inggs, "High resolution SAR processing using stepped-frequencies," *IEEE IGARSS '97*, 490–492, Singapore, 1997.
23. Wilkinson, A. J., R. T. Lord, and M. R.Inggs, "Stepped-frequency processing reconstruction of target reflectivity spectrum," *Communications and Signal Processing, 1998, COMSIG '98*, 101–104, Sept. 1998.
24. Wahlen, A., H. Essen, and T. Brehm, "High resolution millimeterwave SAR," *European Radar Conference*, 217–220, Amsterdam, 2004.
25. Schimpf, H., A. Wahlen, and H. Essen, "High range resolution by means of synthetic bandwidth generated by frequency-stepped chirps," *Electronics Letters*, Vol. 39, No. 18, 1346–1348, Sept. 2003.
26. Bai, X., S.-Y. Mao, and Y.-N. Yuan, "Time domain synthetic bandwidth methods: A 0.1 m resolution SAR technique," *Acta Electronica Sinica*, Vol. 343, No. 3, 472–477, Mar. 2006.
27. Carrara, W. G., R. S. Goodman, and R. M. Majewski, *Spotlight Synthetic Aperture Radar: Signal Processing Algorithms*, Artech House, Norwood, MA, 1995.